

© © 2015 IEEE. Personal use of this material is permitted. Permission from IEEE must be obtained for all other uses, in any current or future media, including reprinting/republishing this material for advertising or promotional purposes, creating new collective works, for resale or redistribution to servers or lists, or reuse of any copyrighted component of this work in other works.

Title: A Model-Based Technique for the Automatic Detection of Earth Continental Ice Subsurface

Targets in Radar Sounder Data

This paper appears in: IEEE Geoscience and Remote Sensing Letter

Date of Publication: 17 April 2014

Author(s): A.M. Ilisei, L. Bruzzone

Volume: 11, Issue 11

Page(s): 1911 – 1915

DOI: 10.1109/LGRS.2014.2313858

A Model-Based Technique for the Automatic Detection of Earth Continental Ice Subsurface Targets in Radar Sounder Data

Ana-Maria Ilisei, *Student Member, IEEE*, and Lorenzo Bruzzone, *Fellow, IEEE*

Abstract

The continuous melting of the ice at the Earth continental polar caps highlights the importance of an exhaustive study of the properties of the ice subsurface targets in order to provide a reliable analysis of their past and future evolution. Such study can be efficiently performed by automatically analysing radargrams of the ice cross-section acquired by radar sounder (RS) instruments. In this paper, we propose an automatic technique for a large scale detection of the ice subsurface targets and the estimation of their properties (e.g., layered area thickness, bedrock scattering area) from radargrams acquired by RS operated at the Earth continental polar caps. This is done by using the parameters of the RS acquisition system combined with the output of an automatic image segmentation algorithm. The segmentation operation is applied to the radargrams after a preliminary processing phase aimed to emphasize the relevant subsurface targets. The segmentation criterion considers the radar signal backscattering properties and a model of the spatial distribution of the investigated targets that takes into account the effects of the wave propagation through the subsurface. Experimental results obtained on real radargrams acquired by an airborne RS in Antarctica confirm the effectiveness of the proposed technique.

Index Terms

Radar sounding, ice thickness, bedrock detection, subsurface analysis, signal processing.

I. INTRODUCTION

The study of the continental subglacial environment is essential for analysing the past and future evolution of the ice subsurface dynamics and its impact on the balance of the ecosystem. Over the past decades, such studies have been carried out by analysing the properties of the ice from radargrams (or echograms) acquired by dedicated radar sounder (RS) instruments. RSs are active instruments that can perform non-intrusive measurements of the subglacial environment by transmitting with a nadir-looking geometry low-frequency electromagnetic waves. At each coordinate of the platform, the presence of dielectric discontinuities in the ice subsurface structure determines the reflection of the wave whose power is measured by the RS receiver and then recorded in the radargram. Radargrams are characterized by relatively fine azimuth and range resolution, therefore allowing for reliable studies of the subsurface. At the continental polar caps, RSs are operated on airborne platforms which enable a significant spatial coverage of the investigated areas and imply the acquisition of a considerable quantity of RS data. In such a large context, it is necessary to use efficient tools for extracting the information conveyed in radargrams. However,

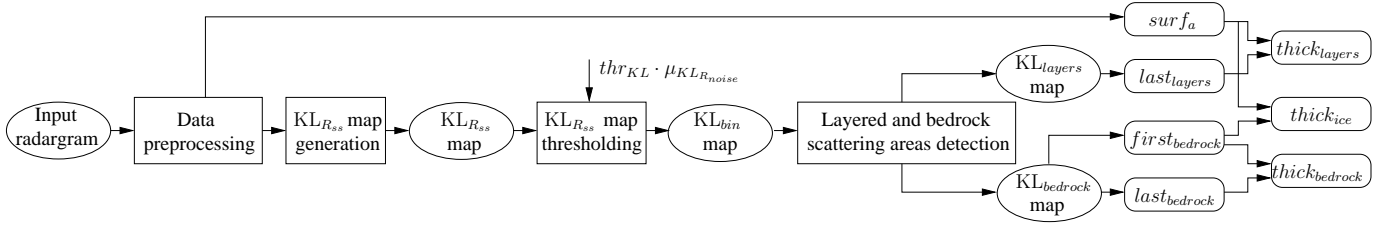


Fig. 1. Block scheme of the proposed technique.

over the past decades, the main approach to the analysis of radargrams has been through either manual investigation or elementary semi-automatic techniques. These approaches are highly inappropriate for the usage of available RS data, since they are time-consuming, inherently subjective and provide qualitative output. These issues call for developing and validating automatic techniques, which can provide fast, quantitative and reliable scientific results, useful for the investigation of the ice subsurface at global scale.

A review of the relative literature points out that techniques for the automatic analysis of the ice subsurface targets have been mainly developed for the analysis of radargrams acquired by orbiting RS on Mars, e.g., [1], [2], [3]. However, due to the different resolution, types of investigated targets, as well as the different processing applied to martian RS data (e.g., on-board presuming used to reduce the volume and thus the quality of data to be downlinked) these algorithms are generally not suitable for an accurate analysis of the ice subsurface from radargrams acquired at the Earth continental polar caps. Nevertheless, such works along with recent advances in the processing of Earth RS data (e.g., [4]), can represent a reliable starting point for the development of advanced automatic techniques for the investigation of RS data.

In this letter we propose a novel unsupervised technique for the automatic detection of ice subsurface targets and the estimation of their properties, which can guarantee quantitative and large scale analysis of radargrams. The proposed technique relies on the knowledge of the statistical properties of the radar signal and the spatial distribution of the subsurface targets. In order to understand the radar signal fluctuations, a preliminary statistical analysis of the radar signals is carried out. Based on such an analysis, the technique generates a statistical map which is afterwards segmented into homogeneous regions corresponding to the different types of targets. The segmentation criterion involves the strength of the signal with respect to noise and a model of the spatial distribution of the subsurface targets (which considers the effects of the wave propagation through the material). The segmentation enables the automatic identification of both the layers and bedrock scattering areas and thus the analysis of their properties. The effectiveness of the proposed technique has been confirmed by results obtained by applying the algorithm to Multichannel Coherent Radar Depth Sounder (MCoRDS) data acquired by the Center for Remote Sensing of Ice Sheets (CReSIS) in Antarctica [5].

II. DETECTION AND ESTIMATION OF ICE SUBSURFACE TARGETS PROPERTIES

The goal of this paper is to develop an efficient technique for the automatic analysis of radargrams, in particular for the detection and properties estimation of the different ice subsurface targets commonly visible in airborne RS data. The architecture of the proposed technique is shown in Fig. 1 and consists of four main blocks: 1) data preprocessing (radargram alignment), 2) statistical map generation, 3) statistical map thresholding, and 4) layered and bedrock scattering areas detection. The blocks

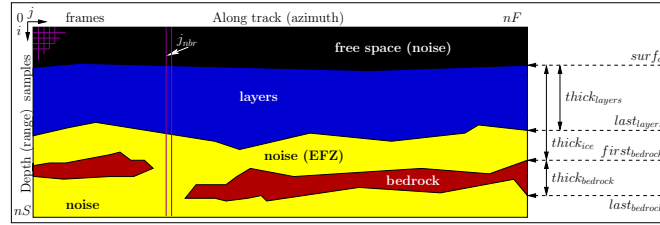


Fig. 2. Model of radargram acquired at the continental polar caps.

of the proposed scheme are detailed in the following subsections, after the description of the model of a typical radargram acquired at the continental polar caps. This model is useful for understanding the types of investigated targets and drives the development of the proposed algorithm.

A. Radargram model

A radargram is a 2D matrix with nS rows (samples i) \times nF columns (frames j) that contains the power of the echoes coming from the ice subsurface and measured by the RS receiver. Such measurements are digitally recorded by exploiting the movement of the platform in the azimuth direction (x-Axis) and an appropriate range sampling frequency f_r of the time intervals between wave transmission and reception (y-Axis). Fig. 2 shows a typical model of a radargram, which highlights the ice subsurface targets to be investigated, i.e., i) *layers* of ice that are spatially coherent englacial surfaces, ii) the *bedrock* scattering area, which represents the portion below the ice/terrain interface within which the backscattered wave has still sufficient power to be measured, and iii) *noise* regions characterized by the absence of scatterers, which are present above and below the bedrock. Note that discontinuities can be present in the bedrock scattering area shown in radargrams (see frame j_{nbr} in Fig. 2). This is not consistent with the real situation in which the terrain under the ice column is expected to be continuous. The reason for this discontinuity is either the loss of power through the ice column or the preprocessing of the radargrams (e.g., which does not completely remove the surface clutter). The noise region located below the bedrock is due to strong attenuation through the subsurface which makes it impossible to acquire coherent returns. Therefore, at the corresponding depth the RS mainly measures noise. According to recent studies [6], the noise region located above the bedrock, also called echo free zone (EFZ), is a consequence of the lack of coherent reflecting surfaces due to the layer disturbances caused by the ice flow at the basal interface. It is worth mentioning here that the main assumption considered in the development of our technique is the presence of the EFZ. This is a reasonable hypothesis as the EFZ is present in extended areas of Antarctica and Greenland [6].

B. Data preprocessing

The instability of the platform that carries the RS introduces errors in the radargram acquisition process, which must be corrected in order to perform accurate analyses of the subsurface targets. These errors are mainly due to the variable height of the platform, which causes the surface and subsurface returns recorded in radargram to appear at range positions that do not correspond to the real air/ice surface and subsurface. In order to correct these displacements, we apply to the radargram a sequence of standard preprocessing steps that consist in a shift in range of the frames of the original radargram. The shifting

operation uses the information provided in the original radargram (i.e., the amplitude data), the knowledge of the elevation of the platform at each acquisition coordinate $j \in [1, nF]$ and the 2-way travel time $time(i)$ between the wave transmission and reception from each sample $i \in [1, nS]$. The output of the preprocessing step is a radargram which is aligned with respect to the WGS84 system. After the alignment, we identify and focus the successive analysis on the subsurface region R_{ss} , which is defined as:

$$R_{ss} = \{i : i > surf_a(j) \wedge i < nS_{ss}, \forall j\} \quad (1)$$

where $surf_a$ is the surface position in the aligned radargram (detected on each frame as the position of the sample with the highest amplitude x , i.e., $surf_a(j) = \arg \max_i \{x(i, j)\}$) and $nS_{ss} = \arg \max_i \{depth(i) \leq d_{ref}\}$ is the sample position corresponding to a depth of d_{ref} (d_{ref} is a reference depth value (e.g., 3500 m) below which the RS typically measures only noise). The depth $depth(i)$ of the subsurface samples is computed according to $depth(i) = c \cdot time(i) / [2 \cdot \sqrt{\epsilon_r}]$, where $c = 3 \cdot 10^8$ [m/s] is the light velocity in free space and $\epsilon_r = 3.15$ is the dielectric permittivity of the ice.

C. Proposed technique

The ice subsurface target properties to be estimated by the proposed technique are: the layer thickness zone $thick_{layers}$ [m] (see (2)), the ice column extension $thick_{ice}$ [m] (which contains both the layer thickness zone and the EFZ) (see (3)) and the bedrock scattering area extension $thick_{bedrock}$ [m] (see (4)). Note that the technique is frame-based and $thick_{ice}$ can be computed only for the frames $j \neq j_{nbr}$, where j_{nbr} indicates the frames with no bedrock returns (see Fig. 2). These properties are estimated as follows:

$$thick_{layers}(j) = [last_{layers}(j) - surf_a(j)] \cdot d_{ss}, \forall j, \quad (2)$$

$$thick_{ice}(j) = [first_{bedrock}(j) - surf_a(j)] \cdot d_{ss}, \forall j \neq j_{nbr}, \quad (3)$$

$$thick_{bedrock}(j) = \begin{cases} [last_{bedrock}(j) - first_{bedrock}(j)] \cdot d_{ss}, & \forall j \neq j_{nbr}, \\ 0, & \forall j = j_{nbr}, \end{cases} \quad (4)$$

where $d_{ss} = c / (2 \cdot f_r \cdot \sqrt{\epsilon_r})$ is the resolution of the pixel in the range direction in the subsurface region, $last_{layers}(j)$ represents the last return of the layered scattering area, and $first_{bedrock}(j)$ and $last_{bedrock}(j)$ are the first and the last returns of the bedrock, respectively, on the j -th frame of the radargram. The borderlines $last_{layers}$, $first_{bedrock}$ and $last_{bedrock}$ are identified by combining the knowledge of the strength of the radar signal with an image segmentation technique that we apply to a statistical map of the subsurface, as explained in the following subsections.

1) *Statistical map generation*: In order to detect the ice subsurface targets we define a segmentation algorithm that can divide the radargram into the three investigated target classes, i.e., *layers*, *bedrock* and *noise*. Given that the radar signals are typically very noisy, we apply the segmentation algorithm to a processed version of the aligned radargram, which we call statistical $KL_{R_{ss}}$ map. The $KL_{R_{ss}}$ map is generated by applying to the R_{ss} region the Kullback-Leibler (KL) divergence [7], which computes the local statistical difference between two distributions. The KL distance is computed between the distribution

of the amplitude samples H inside windows of size $W_r \times W_a$ (range \times azimuth) and the theoretical distribution of the noise N , as follows:

$$\text{KL}(H, N) = \sum_{x_i \in W_r \times W_a} H(x_i) \log [H(x_i)/N(x_i)]. \quad (5)$$

N has been estimated by considering exclusively noise samples, i.e., samples drawn from the bottom part R_{noise} of the aligned radargram (below 3500 m), which is free of target returns and acquisition artifacts (e.g., closure of the acquisition window, double bounce returns of the wave with the surface and platform). These samples have been used for deriving the parameters of the theoretical model of the noise, after a detailed statistical analysis of the radar signal in this region. The statistical analysis has been carried out according to the approach proposed in [1], by fitting to the real distribution of the samples of R_{noise} different theoretical models, i.e., Rayleigh, Gamma, K, Nakagami. The best fitting model has been chosen automatically by minimizing the KL divergence between each fitting model and the real histogram of the amplitude samples considered. After applying this technique to several different radargrams, we concluded that the noise samples can be modeled with a Gamma distribution G_{pdf} characterized by the scale α and shape β parameters, i.e., [8]:

$$G_{pdf} = \left(\frac{x}{\alpha}\right)^{\beta-1} \cdot \frac{e^{-\frac{x}{\alpha}}}{\alpha\Gamma(\beta)}, \quad (6)$$

where $\Gamma(\cdot)$ is the Gamma function. The estimated values of $\hat{\alpha}$ and $\hat{\beta}$ parameters characterizing the Gamma distribution (N in (5)) are computed by using the Maximum Likelihood (ML) estimation approach [8].

The $\text{KL}_{R_{ss}}$ map has been generated by computing (5) and sliding the $W_r \times W_a$ window inside the R_{ss} region. The $\text{KL}_{R_{ss}}$ map is of particular interest as it highlights the most scatterable targets, i.e., whose strength is noticeable higher than that of the noise. This characteristic is going to be considered in the thresholding step. Note that if the input radargram has not been preprocessed for surface clutter return suppression, the $\text{KL}_{R_{ss}}$ map also highlights artifacts due to possible clutter returns [1]. Therefore, a postprocessing step is required to remove clutter.

2) *Statistical map thresholding*: The objective in this step is to extract the regions of the $\text{KL}_{R_{ss}}$ map that have high backscattering, i.e, *layers* and *bedrock*, and to distinguish them from the areas that have low backscattering (only *noise*). To achieve this, we threshold the $\text{KL}_{R_{ss}}$ map on the basis of the mean $\mu_{\text{KL}_{R_{noise}}}$ of the samples of the $\text{KL}_{R_{noise}}$ (which has been generated by applying (5) to R_{noise}), as follows:

$$\text{KL}_{bin}(i, j) = \begin{cases} 1, & \text{if } \text{KL}_{R_{ss}}(i, j) \geq thr_{\text{KL}} \cdot \mu_{\text{KL}_{R_{noise}}} \\ 0, & \text{otherwise} \end{cases} \quad (7)$$

where thr_{KL} is a user defined threshold that controls the degree of similarity between the samples of $\text{KL}_{R_{ss}}$ map and those of $\text{KL}_{R_{noise}}$ map, and KL_{bin} is the binary map (obtained by thresholding the $\text{KL}_{R_{ss}}$ map) that points out the returns corresponding to the *layers* and *bedrock* scattering areas.

3) *Layered and bedrock scattering areas detection*: The aim of this step is to distinguish the returns of the *layers* from those of the *bedrock* region in the KL_{bin} map. In order to perform this operation, we consider the assumption of the presence of the EFZ in the aligned radargram, and implicitly in the $\text{KL}_{R_{ss}}$ and KL_{bin} maps. Therefore, we take into account the spatial

distribution of the subsurface targets and their relational properties, i.e, the expected order of the ice subsurface targets in the range direction: *layers*, *noise* (EFZ), *bedrock* and *noise*. According to this hypothesis, the KL_{bin} map is composed of at least two main disjunct regions, separated by the EFZ, where the one just below the surface $surf_a$ represents the *layers*, and the remaining represent the *bedrock* returns (see Fig. 2). It follows that the region of KL_{bin} map that intersects $surf_a$ contains the returns of the layers (which we represent in the KL_{layers} map), while the remaining regions with value “1” contain only *bedrock* returns (which we represent in the $KL_{bedrock}$ map).

At this point, the frames with no bedrock returns j_{nbr} are those for which there is no value of “1” on the $KL_{bedrock}$ map. For all other frames $j \neq j_{nbr}$, the first return of the bedrock $first_{bedrock}(j)$ is detected as the position of the first “1” encountered by moving downwards over the frames of the $KL_{bedrock}$ map, i.e.,

$$first_{bedrock}(j) = \arg \min_i \{KL_{bedrock}(i, j) = 1\}, \forall j \neq j_{nbr}. \quad (8)$$

Similarly, the last return of the bedrock $last_{bedrock}$ (see (9)) and of the layers $last_{layers}$ (see (10)) are detected as the position of the first “1” found by moving upwards over the frames of the $KL_{bedrock}$ map and KL_{layers} map, respectively.

$$last_{bedrock}(j) = \arg \max_i \{KL_{bedrock}(i, j) = 1\}, \forall j \neq j_{nbr}, \quad (9)$$

$$last_{layers}(j) = \arg \max_i \{KL_{layers}(i, j) = 1\}, \forall j. \quad (10)$$

It is worth noting that on the frames with no bedrock returns j_{nbr} , the computation of bedrock thickness provides $thick_{bedrock}(j_{nbr}) = 0$ (see (4)). Moreover, the EFZ and implicitly the ice thickness $thick_{ice}(j_{nbr})$ (see (3)) cannot be reliably computed. Note that this is not a limitation of the proposed technique, but rather a consequence of the lack of information in the radargram. Approximate values of $thick_{ice}(j_{nbr})$ could be estimated by considering further assumptions (e.g., in the real scenario the terrain is expected to be continuous) and using the detected borderlines at the nearest adjacent frames $j \neq j_{nbr}$.

III. EXPERIMENTAL RESULTS

We applied the proposed technique to a dataset made up of 8 MCoRDS radargrams acquired in sequence over an extension of about 400 km in Antarctica [5]. The data are compressed in azimuth with a Synthetic Aperture Radar (SAR) procedure (for azimuth resolution improvement) and processed according to the minimum variance distortionless response (MVDR) technique (for clutter return suppression) [9]. The resolution of the radargram is 13 m in range, 25 m in azimuth and 70 m in the across-track direction. The range sampling frequency of the instrument is $f_r = 9.5$ MHz, implying $d_{ss} = 8.9$ m.

Since the MCoRDS dataset is composed of radargrams acquired in sequence, in order to align the frames of the radargrams with respect to a single reference frame and to use the information at the lateral borders of the radargrams, we created an extended radargram by appending all the 8 radargrams. We applied the preprocessing steps detailed in Sec. II-B to the extended radargram, thus obtaining an aligned radargram [$nS_{ss} = 410 \times nF = 27350$]. Fig. 3(a) shows a portion [410×3500] of the aligned radargram. The corresponding statistical $KL_{R_{ss}}$ map generated with the algorithm presented in Sec. II-C1 is shown in Fig. 3(b). The size of the sliding window used in the computation of the related $KL_{R_{ss}}$ statistical map has been chosen by

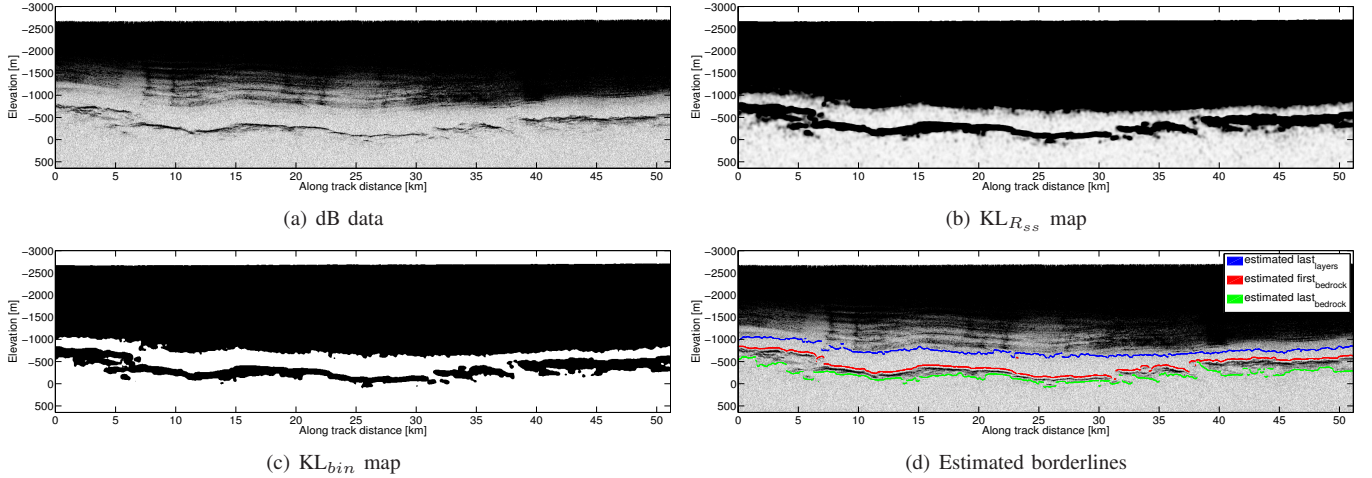


Fig. 3. (a) Example of aligned radargram (dB data). The portion of radargram considered $[410 \times 3500]$ represents a segment on the ground of about 50 km. (b) Corresponding $KL_{R_{ss}}$ statistical map. (c) Corresponding KL_{bin} map. (d) Results provided by the proposed algorithm.

considering the spatial distribution of the subsurface targets, which are mostly extended in the azimuth direction and present sharper variations in the range direction. To account for these variations, we set $W_a = 14$ and $W_r = 7$ samples. For the segmentation of the statistical map we considered values of the threshold $thr_{KL} > 0$. The choice of such value strongly affects the output of the thresholding operation. Indeed, thr_{KL} defines the boundary on the degree of similarity between the samples with high backscattering and samples of noise. Too high values of thr_{KL} may lead to identify samples belonging to high backscattering areas as noise samples, whereas too low values of thr_{KL} may lead to confuse high backscattering samples in the noise regions with *layers* or *bedrock* returns. Fig. 3(c) shows the corresponding KL_{bin} map generated with the proposed algorithm when $thr_{KL} = 10$. Fig. 3(d) shows the position of the $last_{layers}$, $first_{bedrock}$ and $last_{bedrock}$ borderlines detected with the proposed algorithm, for the portion of radargram shown in Fig. 3(a). The output of the proposed algorithm on other three portions of the aligned radargram is provided in Fig. 4.

From a quantitative point of view, since no ground truth data are available for our detection problem, in order to validate the proposed algorithm we created by visual interpretation a reference map of the ice subsurface (i.e., accurate masks of the investigated target classes), from which we picked randomly 200,000 samples (111,946 samples of *layers*, 11,615 samples of *bedrock* and 76,439 samples of *noise*). Tab. I reports the accuracy in the detection of *layers* and *bedrock* scattering areas, in terms of missed and false alarms. Fig. 5 shows the fitting performances of the detection of the three detected borderlines with the reference borders (derived manually) for the portion of radargram shown in Fig. 3(a).

By analyzing the quantitative and qualitative results one can observe that in most of the cases the proposed algorithm detects the targets of interest accurately. The few errors are mainly due to the sliding window approach employed, which tends to filter out some returns, mainly in the regions with low backscattering (e.g., the *bedrock* region). This effect, combined with the thresholding operation, leads to a slight increase in the missed alarm rate. However, the low values of overall errors confirm the effectiveness of the proposed technique.

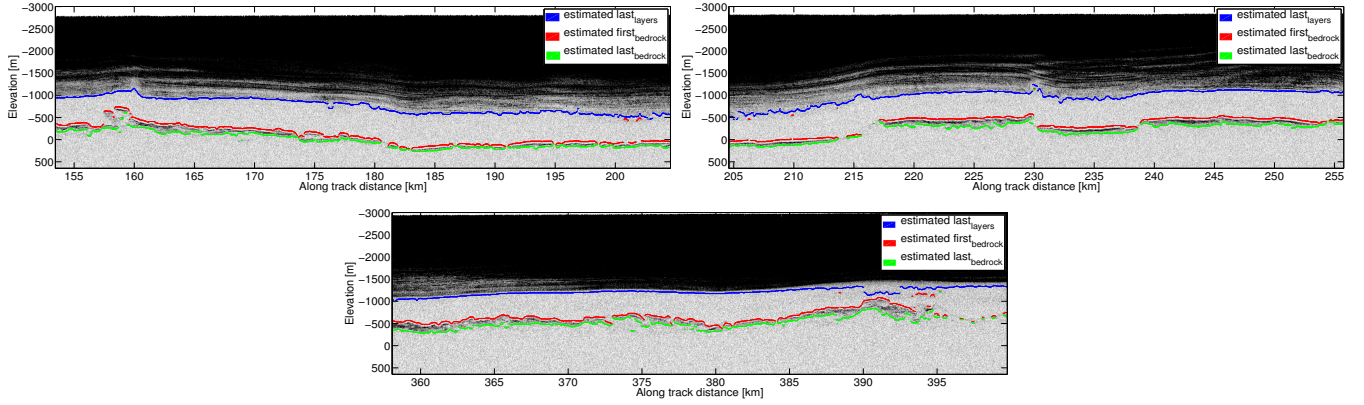


Fig. 4. Example of results provided by the proposed algorithm on three different portions of the aligned radargram.

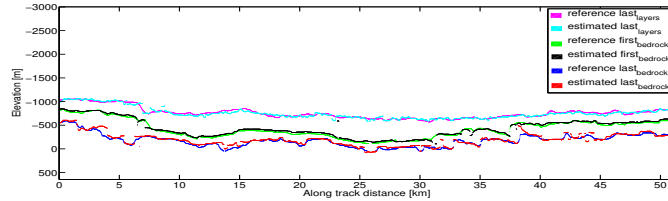


Fig. 5. Example of fitting performances for the $last_{layers}$, $first_{bedrock}$ and $last_{bedrock}$ borderlines for the portion of radargram shown in Fig. 3(a).

IV. CONCLUSION

In this paper we have proposed an unsupervised automatic technique for the detection of the ice subsurface targets and the estimation of their properties from radargrams acquired at the Earth continental polar caps. The main novel contributions of the proposed technique are: i) it is defined on the basis of a realistic model of radargrams that considers the effects of the wave propagation through the ice subsurface (i.e., the presence of the EFZ and the discontinuous shape of the bedrock scattering area), and ii) it involves a segmentation algorithm that enables the detection of both the whole layer area, the ice column (containing also the EFZ) and the bedrock scattering area. The accurate results obtained by applying the proposed technique to real data acquired by an airborne RS in Antarctica are very promising and prove its effectiveness for the analysis of ice subsurface on a large scale.

As future development of this work, we aim to include in the proposed technique an algorithm for the mitigation of surface clutter returns highlighted in the $KL_{R_{ss}}$ map in the final detection results.

ACKNOWLEDGMENT

We acknowledge the use of data and/or data products from CReSIS generated with support from NSF grant ANT-0424589 and NASA grant NNX10AT68G. The authors would also like to thank P. Gogineni [5] for publishing the data and the Italian Space Agency (ASI) for partially supporting this work.

REFERENCES

- [1] A. Ferro and L. Bruzzone, "Analysis of radar sounder signals for the automatic detection and characterization of subsurface features," *IEEE Transactions on Geoscience and Remote Sensing*, vol. 50, no. 11, pp. 4333–4348, November 2012.

TABLE I
ACCURACY PROVIDED BY THE PROPOSED TECHNIQUE FOR THE DETECTION OF LAYERS AND BEDROCK SCATTERING AREAS.

Target class	Target samples	Missed alarms	% Missed alarms	Non-target samples	False alarms	% False alarms	Total error	% Total error
layers	111,946	1,074	0.96	88,054	923	1.05	1,997	0.99
bedrock	11,615	2,120	18.25	188,385	1,344	0.71	3,464	1.73

- [2] G. Freeman, A. Bovik, and J. Holt, "Automated detection of near surface Martian ice layers in orbital radar data," in *IEEE Southwest Symposium on Image Analysis Interpretation (SSIAI)*, May 2010, pp. 117–120.
- [3] A. Ferro and L. Bruzzone, "Automatic extraction and analysis of ice layering in radar sounder data," *IEEE Transactions on Geoscience and Remote Sensing*, vol. 51, no. 3, pp. 1622–1634, 2013.
- [4] C. Gifford, G. Finyom, M. Jefferson, M. Reid, E. Akers, and A. Agah, "Automated polar ice thickness estimation from radar imagery," *IEEE Transactions on Image Processing*, vol. 19, no. 9, pp. 2456–2469, 2010.
- [5] P. Gogineni, "CReSIS Radar Depth Sounder Data," <http://data.cresis.ku.edu/>, 2012, Digital Media., Lawrence, Kansas, USA.
- [6] R. Drews, "Layer disturbances and the radio-echo free zone in ice sheets," *The Cryosphere*, vol. 3, no. 2, pp. 195–203, 2009.
- [7] J. Lin, "Divergence measures based on the Shannon entropy," *IEEE Transactions on Information Theory*, vol. 37, no. 1, pp. 145–151, January 1991.
- [8] C. Forbes, M. Evans, N. Hastings, and B. Peacock, *Statistical Distributions*. John Wiley and Sons, Inc., 2010.
- [9] J. Li, J. Paden, C. Leuschen, F. Rodriguez-Morales, R. Hale, E. Arnold, R. Crowe, D. Gomez-Garcia, and P. Gogineni, "High-Altitude Radar Measurements of Ice Thickness Over the Antarctic and Greenland Ice Sheets as a Part of Operation IceBridge," *IEEE Transactions on Geoscience and Remote Sensing*, vol. 51, no. 2, pp. 742–754, 2013.